Hindawi
Mathematical Problems in Engineering
Volume 2020, Article ID 4251027, 8 pages
https://doi.org/10.1155/2020/4251027

Research Article

Interval Recognition Algorithm of the Pavement Surface Condition Based on Lagrange Interpolation Method

Ren He and Liwei Zhang

School of Automobile and Traffic Engineering, Jiangsu University, Zhenjiang 212013, China

Correspondence should be addressed to Liwei Zhang; 2111704006@stmail.ujs.edu.cn

Received 6 August 2019; Revised 3 February 2020; Accepted 17 February 2020; Published 27 March 2020

Academic Editor: Xiao-Qiao He

The accurate recognition of road condition is one of the important factors that influence vehicle safety performance. This paper comes up with an original mathematical method of an interval recognition algorithm of the pavement surface condition based on Lagrange interpolation. The ordinate of the peak point is solved by the Lagrange interpolation method, and the pavement surface condition is deduced by the interval identification algorithm. The simulation results from six typical roads and the varied pavement surface show that besides the cobblestone pavement which is not common in the daily road, the estimation error of the initial tire-road friction coefficient by the Lagrange interpolation method is less than 2%, the pavement surface condition can be identified by interval recognition algorithm quickly and accurately, and the response time is less than 0.2 seconds.

1. Introduction

In order to reduce the occurrence of traffic accidents, major automobile companies and research institutes began to research and develop vehicle active safety control technology, such as ABS, TCS, EBD, ESP, and ACC. The essence of these active control strategies is to adjust the force acting on the tire and pavement surface so as to achieve the purpose of braking (driving) control and vehicle stability control, which are restricted by the adhesion conditions between the tire and the pavement surface [1, 2]. For example, the maximum brake deceleration can be provided by a dry asphalt pavement with the adhesion coefficient being about 1, 20 times than that by an ice pavement with the adhesion coefficient being about 0.05. This means that on different pavement surface conditions, the braking distance of the car may be 20 times different, which is crucial to the safe operation of the car.

Besides the quality of active safety control strategy, the significant automated driving depends to a great extent on whether the current road adhesion coefficient can be fully utilized.

The key to improving the utilization ratio of road adhesion coefficient is to obtain the maximum tire-road friction coefficient in real time.

The tire-road friction coefficient μ is defined formally as follows [3]:

$$\mu = \frac{\sqrt{F_x^2 + F_y^2}}{F_z}, \tag{1}$$

where F_z, F_x, and F_y are the normal forces, longitudinal forces, and side forces acting on the tire, respectively. For this wheel, maximum tire-road friction coefficient $\mu_{\max}$ is the maximum achievable value of $|\mu|$.

If we only consider the longitudinal motion of the vehicle, then the side force F_y can be neglected:

$$\mu = \frac{F_x}{F_z}. \tag{2}$$

2. Review of Previous Results

The road recognition method is traditionally examined with "cause-based" approaches and "effect-based" approaches according to the principles of the recognition method [4, 5], as shown in Figure 1.

The "cause-based" strategies try to measure factors that lead to changes in friction and then attempt to predict $\mu_{\max}$

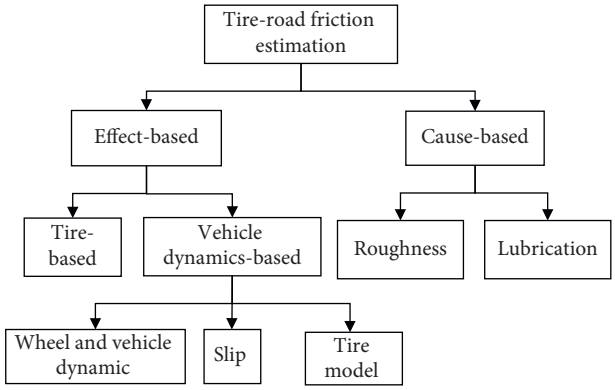

Figure 1: Classification of road recognition methods.

via some additional sensors. The aim of the "cause-based" approach is to find a correlation between the sensor data and tire-road friction-related parameters such as roughness and lubrication of the pavement surface. The most commonly used sensors are optical sensors, cameras [6, 7], and acoustic sensors [8].

The main advantage of the "cause-based" method is that it can identify the pavement surface condition before the vehicle passes, which is of great significance to future pilotless. Besides, this method is not limited by the current road adhesion coefficient and can predict the maximum tire-road friction coefficient precisely under the condition that the friction between the tire roads is low.

However, this method exists two main disadvantages: first, the experiment-based approach considers only the road level and not the tire wear of the vehicle itself. Even on the road with good tire-road friction coefficients, tire with severe tread wear will not get good adhesion, which is very harmful to the control of vehicles after identifying the maximum tire-road friction coefficient.

The second disadvantage is that the experiment-based approach usually requires additional sensors, which are usually expensive and vulnerable to external interference. When the sensor is polluted, it is harmful for the safe driving of the car.

The "effect-based" approach, on the other hand, estimates the tire-road friction coefficient by testing the motion response generated by the change in the road adhesion coefficient on the vehicle body or tire.

It can be divided into tire-based response and vehicle dynamics response to identify the tire-road friction coefficient.

The tire-based response can be further divided into two methods of measuring the tire noise response [9] and measuring the tread deformation [10]. Both of these two methods do not get rid of the drawbacks of requiring additional sensors.

The vehicle dynamics response approaches try to estimate the friction using mathematical models. The most commonly mathematical models are wheel dynamic model [11, 12], roll dynamic model [13], quarter car model [14], four-wheel vehicle model [3], bicycle model [15, 16], and tire model such as Pacejka tire model, Dugoff tire model, and Burckhardt tire model [17].

The vehicle dynamics response approaches do not require additional sensors and the accuracy of the recognition is within the allowable range.

But it still exists disadvantages that usually need to the tire close to locked state, which is harmful to the control of the vehicle, to estimate the maximum tire-road friction coefficient.

Besides the quality of active safety control strategy, proper maintenance of a road network needs to evaluate the pavement surface condition [18].

In order to avoid the problem of high cost and easy to be polluted of the sensor method, and the disadvantage of the model-based method that can identify the maximum tire-road friction coefficient only when the tire is locked in the critical state, an original mathematical method was proposed. The Lagrange interpolation method in mathematics for reference is used to determine the maximum friction coefficient, and an interval recognition algorithm is used to determine the final pavement surface condition.

The organization of this paper is as follows. In Section 3, the system model is explained briefly, which discusses the wheel dynamics model and tire model. Section 4 expounds the overall approach to tire-road friction estimation. In this section, the acquisition of real-time road adhesion coefficient, the calculation of braking torque, and the application of the Lagrange interpolation method are introduced in detail. In Section 5, the simulation results of different roads and the varied pavement surface are given to verify the effectiveness of the algorithm. Finally, the paper ends with conclusion in Section 6.

3. System Model

3.1. Wheel Dynamics Model. Suppose the vehicle runs straight on the horizontal road, ignoring the air resistance and rolling resistance, the single-wheel model is shown as in Figure 2.

This model assumes that the normal load is considered to be small and ignorable, and the dynamic differential equations are described as follows:

$$\begin{cases} J\dot{\omega} = F_x R - T_b, \\ m\dot{V} = F_x, \\ F_x = \mu(s) F_z, \\ F_z = mg, \end{cases} \tag{3}$$

where J is the wheel inertia, ω is the wheel angular velocity, T_b is the braking torque, F_x is the friction force, R is the wheel radius, m is the 1/4 vehicle mass, V is the wheel center speed, and F_z is the vehicle normal load.

Moreover, $\mu(s)$ expresses that the road adhesion coefficient μ is the equation of the slip ratio S, which is specifically introduced in the next section. Consider only the case of braking, the slip ratio S can be written as follows [19]:

$$S = \frac{V - \omega R}{V}. \tag{4}$$

The calculation of the slip ratio S needs to know the wheel center speed V and the wheel angular velocity ω,

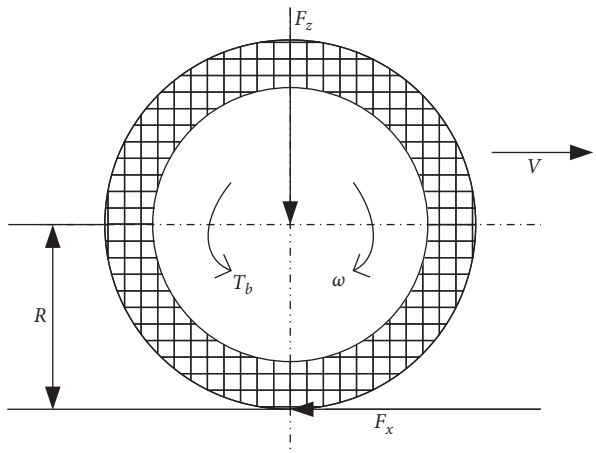

Figure 2: Single-wheel model of vehicle.

which can be obtained by equation (3) after knowing the braking torque T_b and the real-time tire-road friction coefficient μ. Detailed calculation processes of the braking torque T_b and road adhesion coefficient μ are presented in Section 4.

3.2. Tire Model. Compared with Pacejka tire model, Dugoff tire model, and so on, Burckhardt tire model has the advantages of simple formula complexity, fewer parameters, and accuracy within the permissible range [20]. Therefore, in this paper, the Burckhardt tire model which expresses the relationship between seven typical tire-road friction coefficients and slip ratio is adopted. The expression can be written as follows:

$$\mu(s) = \{c_1[1 - \exp(-c_2 s)] - c_3 s\} e^{-c_4 v}, \quad (5)$$

where c_i $(i = 1, \ldots, 4)$ are fitted by experimental data corresponding to different roads. $e^{-c_4 v}$ reflects the change of tire-road friction coefficient caused by the change of the wheel center speed V.

If the influence of velocity change is neglected, the model expression can be simplified as follows:

$$\mu(s) = c_1[1 - \exp(-c_2 s)] - c_3 s, \quad (6)$$

where c_1, c_2, and c_3 for different roads are listed in Table 1 [18, 20].

Figure 3 is drawn according to the data provided in Table 1.

4. Overall Approach to Tire-Road Friction Coefficient Estimation

4.1. Description of Approach. From the observation of Figure 3, we can find that μ is an increasing function of S until reaching a critical slip value, where μ reaches $\mu_{\max}$ and then decreases. Moreover, we can also find that the peak points of other pavement curves are approximately in a straight line with a slope of "K."

If we ignore the "Dry Cobblestone" road, which is not common, the trend of different road curves is more consistent. Therefore, we assume that the road curve equation to be estimated has the same trend of change.

Table 1: Parameter table of the tire model for various roads.

Surface condition	C_1	C_2	C_3
Dry asphalt	1.28	23.99	0.52
Dry cobblestone	1.371	6.46	0.67
Dry cement	1.197	25.17	0.54
Wet asphalt	0.857	33.82	0.35
Wet cobblestone	0.4	33.71	0.12
Snow	0.195	94.13	0.0646
Ice	0.05	306.39	0.001

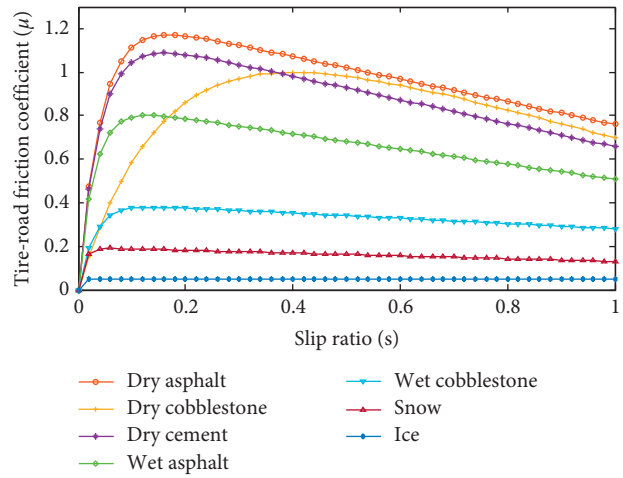

Figure 3: $\mu(s)$ curves of typical roads.

Based on this idea, we hope to find the relationship between peak points of various known typical road curves first. Then, an original mathematical method is proposed as is shown in Figure 4:

First, we get the straight line whose slope is "K," which is fitted by the peak point of typical road curve ("Oblique line 1" in Figure 4). Suppose "Curve 1" is the road curve which we need to estimate, and point "$b0$" is the known point on "Curve 1." Then, we can find a straight line ("Oblique line 2" in Figure 4) whose slope is "K" across "$b0$."

Furthermore, we can easily find the intersection "$b1 \sim b6$" of "Oblique line 2" with six other known typical road curves. Using the Lagrange interpolation method, we can express the relationship between "$b0$" and b_i $(i = 1, \ldots, 6)$, which is the relationship between "Curve 1" and six known typical road curves.

Since the variation trend of each road curve is same, we can reverse the ordinate value of the peak point "$a0$" of "Curve 1" when this relationship and the coordinates of the peak points of the six typical roads are known.

Finally, based on the interval in which the ordinate value of "$a0$" located, the type of pavement surface that needs to be estimated can be determined.

After knowing the type of pavement surface, we can easily get the maximum tire-road friction coefficient $\mu_{\max}$ through the Burckhardt tire model.

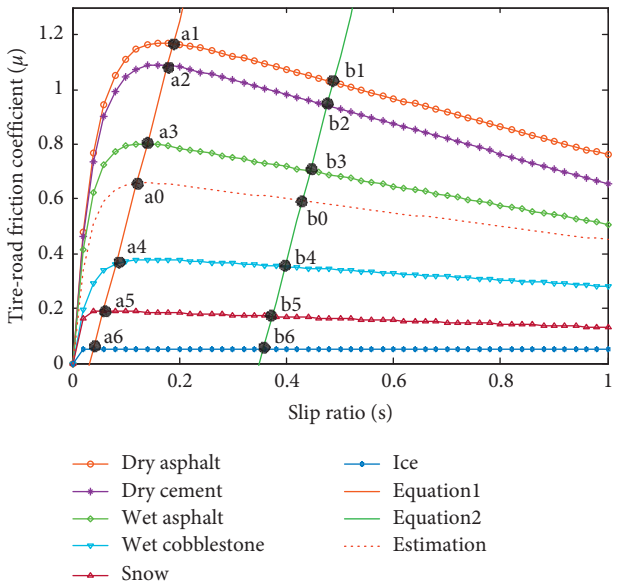

Figure 4: Schematic diagram of the tire-road friction coefficient estimation method.

It should be noted that "Oblique line 1" in Figure 4 is fitted by the peak coordinates of known typical road curves. In this paper, the coordinate values of "$a1 \sim a6$," which are the intersection of "Oblique line 1" and the other six typical road curves, are approximate to the coordinate values of six typical road curves at the peak point.

The overall approach used in this paper for the estimation of pavement surface condition consists of the following four steps:

(1) Solve the straight line equation fitted by the peak points of six typical road curves.

(2) Solve the real-time tire-road friction coefficient and real-time slip ratio.

(3) Solve the ordinate value of the peak point "$a0$" using Lagrange interpolation.

(4) Determine the pavement surface condition utilization recognition interval.

Firstly, the linear equation whose slope is "K" is obtained by fitting data points, which are the coordinates of peak points calculated from different typical road curves. In the second step, the observer and the wheel dynamics model are used to solve real-time road friction coefficient and real-time slip ratio, respectively. In step 3, the Lagrange interpolation method is used to obtain the ordinate value of the peak point "$a0$." Finally, based on the pavement surface recognition interval in which the ordinate value of "$a0$" located, the pavement surface condition is determined. The detailed introduction is as follows.

4.2. Solution of the Linear Equation. As described in 4.1, the line with a slope of "K" is fitted by the vertices of a typical road curve. In order to find out the linear equation, we need to find out the coordinate of the peak point of the typical road curve first.

By using the method of finding the extremism, the derivative of equation (6) for S can be obtained:

$$\mu_{\max} = c_1 + \frac{c_3}{c_2}\left(\ln\frac{c_3}{c_1 c_2} - 1\right). \tag{7}$$

The maximum tire-road friction coefficient $\mu_{\max}$ and the optimal slip ratio S_0 which is the coordinate value of the peak point of the typical road curve are obtained, respectively, as shown in Table 2.

"Oblique line 1" can be obtained by fitting the points in Table 2. The diagram of "Oblique line 1" is displayed in Figure 5.

The expression of the fitting equation "Oblique line 1" is

$$f(x) = 7.484x - 0.2498. \tag{8}$$

In this paper, the intersection of "Oblique line 1" and the other six typical road curves are approximate to the coordinate values of six typical road curves at the peak point.

4.3. Solution of the Real-Time Tire-Road Friction Coefficient. In order to achieve real-time road adhesion coefficient, the state observer is designed. Via equation (3), we can get

$$\dot{\omega} = \frac{\mu F_z R - T_b}{J} = -\frac{T_b}{J} + \frac{mgR}{J}\mu. \tag{9}$$

It is a first-order nonlinear system of the wheel brake, in which the braking torque T_b is the control input and the wheel speed ω is the system output. The item with the tire-road friction coefficient $(mgR/J)\mu$ can be considered as additional interference f, which is the expansion state variable of the system.

Replace the following equation as

$$\begin{cases} x_1 = \omega, \\ x_2 = f = \dfrac{mgR}{J}, \\ u = T_b, \\ b = -\dfrac{1}{J}. \end{cases} \tag{10}$$

Equation (9) can be transformed into the following form:

$$\begin{cases} \dot{\hat{x}}_1 = bu + \hat{x}_2 + \dfrac{\alpha_1}{\varepsilon}(x - \hat{x}_1) \\ \dot{\hat{x}}_2 = \dfrac{\alpha_1}{\varepsilon^2}(x - \hat{x}_1), \end{cases} \tag{11}$$

where $\hat{x}_1$ and $\hat{x}_2$ are the observed values of x_1 and x_2, respectively, u and x are the input, $\hat{x}_1$, $\hat{x}_2$ are the output value of the state observer, $\varepsilon > 0$, and α_1 and α_2 are both positive real numbers.

Once the braking torque and angular velocity are known, the real-time tire-road friction coefficient can be obtained by the designed observer. The value of angular velocity is measured by the vehicle angular velocity sensor which is well equipped, and the calculation method of braking torque is introduced in next section.

Table 2: Parameter table of maximum tire-road friction coefficient and optimal slip ratio.

Surface condition	μ_{max}	S_0
Dry asphalt	1.17	0.17
Dry cement	1.09	0.16
Wet asphalt	0.8	0.131
Wet cobblestone	0.38	0.14
Snow	0.19	0.06
Ice	0.05	0.031

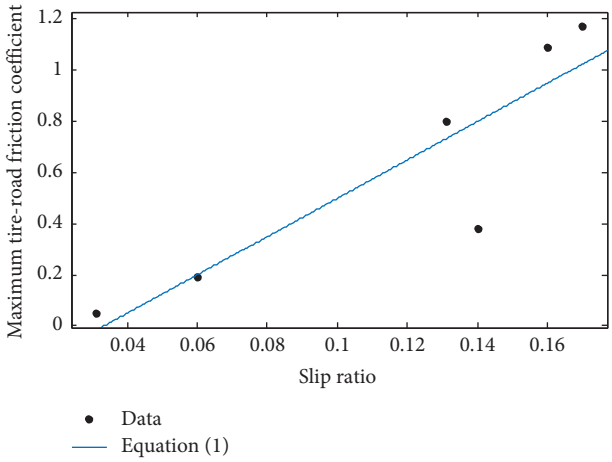

Figure 5: Fitting equation result diagram.

4.4. Solution of the Real-Time Slip Ratio. Through the introduction of the tire dynamics model in Section 3, the slip ratio S can be calculated as long as the braking torque T_b and the real-time tire-road friction coefficient μ are known.

Since μ has been introduced in Section 4.3, the following focuses on the solution of the T_b.

In this paper, the slip ratio S is taken as the control objective, and the sliding mode variable structure control method is selected to control the braking torque.

When the control system moves on the sliding surface, the real-time slip ratio reaches the target slip ratio while keeping the slip ratio constant. Then, $\dot{S} = 0$.

Using equation (4), the expression of $\dot{S}$ is obtained as

$$\dot{s} = \frac{1}{v}(-\dot{\omega}R + (1-s)\dot{v}). \tag{12}$$

Let $\dot{S} = 0$ and bring equation (9) into equation (12) to get the braking torque T_{b1} on the sliding surface as follows:

$$T_{b1} = \mu F_z R + (s-1)\frac{J\dot{V}}{R}. \tag{13}$$

When the control system is outside the sliding surface, it should be controlled to the sliding surface as soon as possible, and the jitter problem should be reduced when the sliding surface is reached. The expression of the exponential approach rate is selected as [21]

$$\dot{s} = \varepsilon \cdot \operatorname{sgn}(s) - ks. \tag{14}$$

By introducing equation (14) into equation (12), the braking torque T_{b2} outside the sliding mode surface can be obtained as

$$T_{b2} = T_{b1} - \frac{JV}{R}(\varepsilon \cdot \operatorname{sgn}(s) + ks). \tag{15}$$

To sum up, we get the expression of braking torque as

$$T_b = \begin{cases} \mu F_z R + (s-1)\dfrac{J\dot{V}}{R}, & \dot{s} = 0, \\ \mu F_z R + (s-1)\dfrac{J\dot{V}}{R} - \dfrac{JV}{R}(\varepsilon \cdot \operatorname{sgn}(s) + ks), & \dot{s} \neq 0. \end{cases} \tag{16}$$

After knowing S and μ which is equal to the coordinate value of "$b0$," the expression of "Oblique line 2" can be obtained by the mathematical method. Then, the intersection coordinates of "Oblique line 2" and six other typical road curves are obtained.

The following is the introduction of the Lagrange interpolation method for obtaining the ordinate value of the peak point "$a0$" of "Curve 1."

4.5. Solution of the Ordinate Value of "a0" by Lagrange Interpolation Method. Just as described in Section 4.1, Lagrange interpolation is mainly used to describe the relationship between curves. Comparing the coordinate value of "$b0$" with each intersection coordinates of "Oblique line 2" and six other typical road curves, we can get the relationship between "Curve 1" and other six typical road curves by the Lagrange interpolation method.

Let λ_i $(i = 1, \ldots, 6)$ represent the relationship between "Curve 1" and six other standard road curves, respectively.

The expression of the basis function of the Lagrange interpolation λ_i $(i = 1, \ldots, 6)$ can be represented as

$$\lambda_i = \frac{(\mu_{b0} - \mu_{b1}) \cdots (\mu_{b0} - \mu_{bi-1})(\mu_{b0} - \mu_{bi+1})}{(\mu_{bi} - \mu_{b1}) \cdots (\mu_{bi} - \mu_{bi-1})(\mu_{bi} - \mu_{bi+1})} \frac{\cdots (\mu_{b0} - \mu_{b6})}{\cdots (\mu_{bi} - \mu_{b6})}, \tag{17}$$

where μ_{bi} $(i = 0, \ldots, 6)$ represent the ordinate value of the point "b_i" $(i = 0, \ldots, 6)$.

According to λ_i $(i = 0, \ldots, 6)$ and the ordinate values of the peak point of six topical road curves (as shown in Table 2), we can get the ordinate value of the point "$a0$," which is the peak point of "Curve 1."

Define that μ_{ai} $(i = 0, \ldots, 6)$ represent the ordinate value of point "a_i" $(i = 0, \ldots, 6)$. Then, the expression of μ_{a0} is as follows:

$$\mu_{a0} = \lambda_1\mu_{a1} + \lambda_2\mu_{a2} + \lambda_3\mu_{a3} + \lambda_4\mu_{a4} + \lambda_5\mu_{a5} + \lambda_6\mu_{a6}. \tag{18}$$

Table 3: Parameter table of recognition interval of the typical pavement surface.

Road number	Surface condition	Interval	Value
1	Ice	$(0, L_1)$	(0, 0.12)
2	Snow	$[L_1, L_2)$	[0.12, 0.285)
3	Wet cobblestone	$[L_2, L_3)$	[0.285, 0.59)
4	Wet asphalt	$[L_3, L_4)$	[0.59, 0.945)
5	Dry cement	$[L_4, L_5)$	[0.945, 1.13)
6	Dry asphalt	$[L_5, L_6)$	[1.13, 1.53)

Table 4: Main parameters of the wheel model.

Parameter	Symbol	Value (kg)
Mass	m	375
Wheel inertia	J	1.5^2
Wheel radius	R	0.26

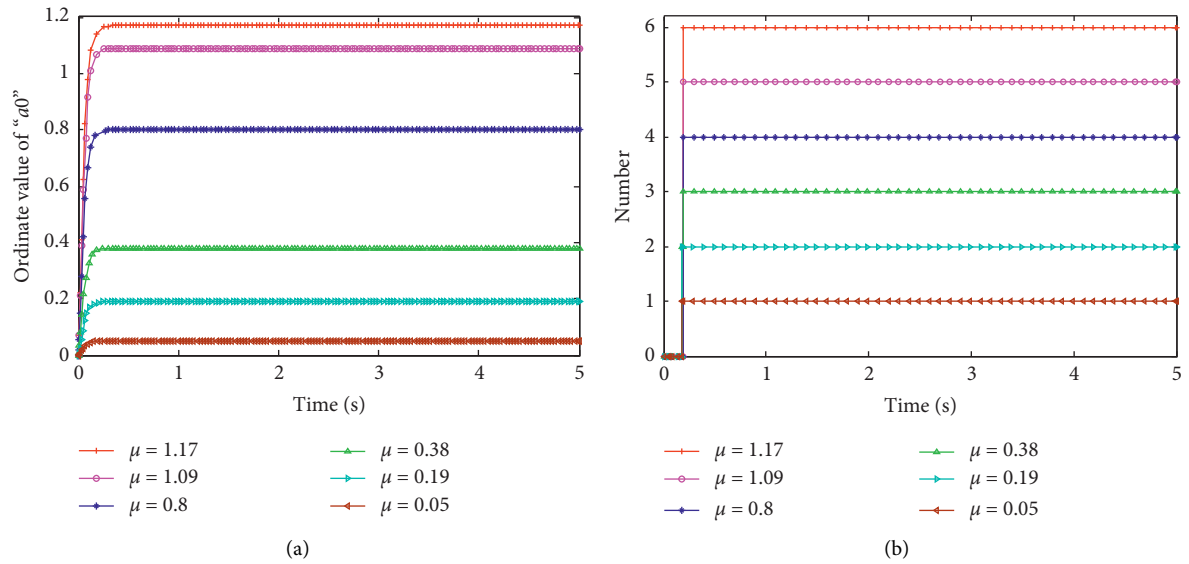

Figure 6: Simulation results of different tire-road friction coefficients. (a) Ordinate value of "$a0$"of different tire-road friction coefficients. (b) Number of different tire-road friction coefficients.

Table 5: Parameter table of ordinate value of "$a0$" and number of different tire-road friction coefficients.

Surface condition	μ	Ordinate value of "$a0$"	Error	Number
Ice	0.05	0.05065	1.3	1
Snow	0.19	0.1925	1.316	2
Wet cobblestone	0.38	0.3985	4.87	3
Wet asphalt	0.8	0.8121	1.51	4
Dry cement	1.09	1.11	1.83	5
Dry asphalt	1.17	1.189	1.62	6

4.6. Determination of the Maximum Tire-Road Friction Coefficient. After obtaining the ordinate value of the peak point "$a0$," we also need to know the pavement surface recognition interval in which the ordinate value of "$a0$" located. Then, the next is a detailed introduction of interval selection.

In order to improve the stability of interval recognition, the average value of the theoretical maximum tire-road friction coefficient of adjacent roads is selected as the boundary of the recognition interval. The calculation equation is as follows:

$$\begin{cases} L_i = \dfrac{\mu_{\max i} + \mu_{\max(i+1)}}{2}, & 1 \le i \le 5, \\ L_6 = L_5 + 0.4, \end{cases} \tag{19}$$

where L_i represents the boundary value of the recognition interval.

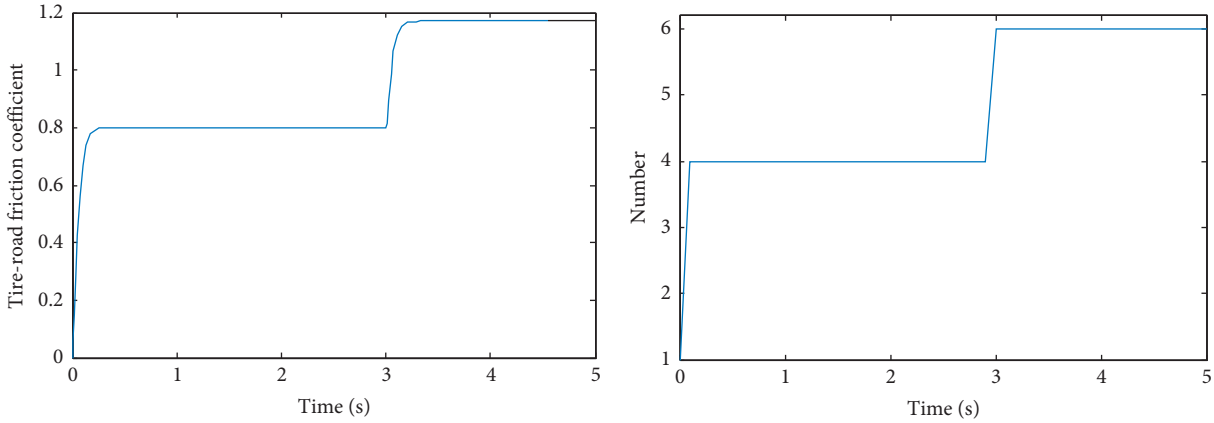

Figure 7: Simulation results of varied pavement surface. (a) Ordinate value of "$a0$"of varied pavement surface. (b) Number of varied pavement surface.

According to equation (19) and Table 2, the recognition interval of the typical pavement surface can be obtained as in Table 3. For the convenience of description, we numbered the pavement surface, respectively, as follows.

5. Simulation and Analysis

Simulation is conducted in the MATLAB/Simulink environment to show the result of the algorithm. The initial vehicle velocity is set at 100 km/h, and the main parameters of the wheel model are shown in Table 4. Figure 6 shows the state responses of simulation.

The ordinate value of "$a0$" and road numbers obtained by the recognition algorithm are shown in Table 5:

It is observed from Table 5 that excluding the error of wet cobblestone is close to 5%, the estimated error of the "$a0$"coordinate by Lagrange interpolation is less than 2%.

The method of solving the ordinate value of "$a0$" by the Lagrange interpolation method can be proved to be effective and has the advantage of requiring fewer data points.

Then, the pavement surface condition can be deduced by the interval identification algorithm based on the recognition interval in which the ordinate value of "$a0$" is located. After identifying the pavement surface condition by the interval algorithm, the type of pavement can be accurately determined.

In order to further verify the effectiveness of the method, the more varied pavement surface was selected for simulation. The selected pavement surface was changed from the asphalt road with an adhesion coefficient of 0.8 to the dry asphalt road with an adhesion coefficient of 1.17. The simulation results are as follows.

According to Figure 7, it can be seen that the pavement surface condition can be accurately identified by the interval recognition algorithm based on Lagrange interpolation, and the response time is less than 0.2 seconds.

6. Conclusion

An original mathematical method of the interval recognition algorithm of road adhesion coefficient based on Lagrange interpolation is presented. The ordinate of the peak point of the road curve to be estimated is solved by the Lagrange interpolation method, and the pavement surface condition is deduced by the interval identification algorithm based on the recognition interval in which the ordinate value of "$a0$" located.

The simulation results from six typical roads show that besides the cobblestone pavement which is not common in the daily road, the estimation error of the ordinate of the peak point by the Lagrange interpolation method is less than 2%, and the pavement surface condition can be accurately identified by the interval recognition algorithm. In addition, the simulation results of the varied pavement surface show that the method can also identify the road type quickly and accurately, and the response time is less than 0.2 seconds. Therefore, the proposed novel mathematical method can not only maintain the accuracy of pavement surface condition estimation but also meet the requirements of the rapid response and have the advantage of requiring fewer data points.

Data Availability

The data used to support the findings of this study are included within the article.

Conflicts of Interest

The authors declare that they have no conflicts of interest.

Acknowledgments

This paper was sponsored by the Chinese National Natural Science Foundation (no. 51875258) and Postgraduate Research and Practice Innovation Program of Jiangsu Province (no. KYCX18_2229).

References

[1] H. Guo, Z. Yin, D. Cao, H. Chen, and C. Lv, "A review of estimation for vehicle tire-road interactions toward automated driving," *IEEE Transactions on Systems, Man, and Cybernetics: Systems*, vol. 49, no. 1, pp. 14–30, 2019.

[2] L. Shao, C. Jin, C. Lex, and A. Eichberger, "Robust road friction estimation during vehicle steering," *Vehicle System Dynamics*, vol. 57, no. 4, pp. 493–519, 2019.

[3] M. Doumiati, A. Charara, A. C. Victorino, and D. Lechner, "Vehicle dynamics estimation using Kalman filtering: experimental validation," *Working Papers*, vol. 14, no. 1, pp. 137–171, 2013.

[4] R. Rajamani, G. Phanomchoeng, D. Piyabongkarn, and J. Y. Lew, "Algorithms for real-time estimation of individual wheel tire-road friction coefficients," *IEEE/ASME Transactions on Mechatronics*, vol. 17, no. 6, pp. 1183–1195, 2012.

[5] S. Muller, "Estimation of the maximum tire-road friction coefficient," *Epilepsy Research*, vol. 108, no. 2, pp. 327–330, 2003.

[6] A. J. Tuononen and L. Hartikainen, "Optical position detection sensor to measure tyre carcass deflections in aquaplaning," *International Journal of Vehicle Systems Modelling & Testing*, vol. 3, no. 3, pp. 189–197, 2008.

[7] A. J. Tuononen, "Optical position detection to measure tyre carcass deflections," *Vehicle System Dynamics*, vol. 46, no. 6, pp. 471–481, 2008.

[8] J. Alonso, J. M. López, I. Pavón et al., "On-board wet road surface identification using tyre/road noise and support vector machines," *Applied Acoustics*, vol. 76, no. 1, pp. 407–415, 2014.

[9] F. Holzmann, M. Bellino, R. Siegwart, and H. Bubb, "Predictive estimation of the road-tire friction coefficient," in *Proceedings of the 2006 IEEE International Symposium on Intelligent Control*, pp. 885–890, Munich, Germany, October 2006.

[10] G. Erdogan, L. Alexander, and R. Rajamani, "Estimation of tire-road friction coefficient using a novel wireless piezoelectric tire sensor," *IEEE Sensors Journal*, vol. 11, no. 2, pp. 267–279, 2011.

[11] T. Hsiao, N. C. Liu, and S. Y. Chen, "Robust estimation of the friction forces generated by each tire of a vehicle," in *Proceedings of the 2011 American Control Conference*, pp. 5261–5266, San Francisco, CA, USA, June 2011.

[12] K. Han, E. Lee, M. Choi, and S. B. Choi, "Adaptive scheme for the real-time estimation of tire-road friction coefficient and vehicle velocity," *IEEE/ASME Transactions on Mechatronics*, vol. 22, no. 4, pp. 1508–1518, 2017.

[13] K. B. Singh and S. Taheri, "Estimation of tire–road friction coefficient and its application in chassis control systems," *Systems Science & Control Engineering*, vol. 3, no. 1, pp. 39–61, 2015.

[14] M. Doumiati, A. Charara, A. C. Victorino, and D. Lechner, "Road safety: embedded observers for estimation of vehicle vertical tire forces," *International Journal of Vehicle Autonomous Systems*, vol. 10, no. 1/2, pp. 117–143, 2012.

[15] K. Han, M. Choi, and S. Choi, "Estimation of tire cornering stiffness as a road surface classification indicator using understeering characteristics," *IEEE Transactions on Vehicular Technology*, vol. 99, p. 1, 2018.

[16] Y. H. Liu, T. Li, Y. Y. Yang, X. W. Ji, and J. Wu, "Estimation of tire-road friction coefficient based on combined APF-IEKF and iteration algorithm," *Mechanical Systems and Signal Processing*, vol. 88, pp. 25–35, 2017.

[17] G. Cui, J. Dou, S. Li, X. Zhao, X. Lu, and Z. Yu, "Slip control of electric vehicle based on tire-road friction coefficient estimation," *Mathematical Problems in Engineering*, vol. 2017, Article ID 3035124, 8 pages, 2017.

[18] P. Zoccali, G. Loprencipe, and A. Galoni, "Sampietrini stone pavements: distress analysis using pavement condition index method," *Applied Sciences*, vol. 7, no. 7, p. 669, 2017.

[19] K. Han, Y. Hwang, E. Lee, and S. Choi, "Robust estimation of maximum tire-road friction coefficient considering road surface irregularity," *International Journal of Automotive Technology*, vol. 17, no. 3, pp. 415–425, 2016.

[20] X. Zhang, F. Wang, and Y. Gao, "Analysis of the tire steady-state models," *Automobile Technology*, vol. 437, no. 2, pp. 1–7, 2012, in Chinese.

[21] J. Liu, *Sliding Mode Control Design and Matlab Simulation*, Tsinghua University Press, Beijing, China, 2005.